These equations show the reason for the differences between the two polarizations: The perpendicular polarization is much more sensitive to the shape of the distribution function than the parallel one. The parameter $b$ in Eq. (5) becomes smaller for high pressures and compensates the decrease of population inversion.

In deriving Eqs. (5) and (6), large-angle electron scattering was neglected although these collisions contribute to amplification more than the small-angle scattering. However, these large-angle collisions are less important in evaluating the small current changes. This is one of the reasons why maximum amplification is closer to the cathode than the maximum of current decrease. Another reason is the recombination effect which is important in the negative glow region. The incident electromagnetic wave reduces the recombination rate between slow electrons and ions (Chen, Leiby, and Goldstein[8]), and this causes a current increase.

Application of the stimulated bremsstrahlung emission for developing a new type of a tunable maser seems quite promising, since it depends neither on relativistic electron beams nor on complicated magnetic fields as is the case in standard free-electron lasers.[9]

It is interesting to note that there was considerable disagreement concerning amplification in a plasma about twenty years ago, especially between Browne[10,11] and Twiss[12,13] over the possibility of maser action in space.

[1]Z. Geller and W. Low, Nature (London) 176, 1021 (1955).
[2]N. M. Kroll and K. M. Watson, Phys. Rev. A 8, 804 (1973).
[3]A. Weingartshofer, J. K. Holmes, G. Caudle, E. M. Clarke, and H. Krüger, Phys. Rev. Lett. 39, 269 (1977).
[4]A. Weingartshofer, E. M. Clarke, J. K. Holmes, and C. Jung, Phys. Rev. A 19, 2371 (1979).
[5]L. Schlessinger and J. Wright, Phys. Rev. A 20, 1934 (1979).
[6]H. S. W. Massey, E. H. S. Burhop, and H. B. Gilbody, *Electronic and Ionic Impact Phenomena* (Clarendon, Oxford, 1969), 2nd ed., Vol. I, p. 48.
[7]D. F. Register, S. Trajmar, and S. K. Srivastava, Phys. Rev. A 21, 1134 (1980).
[8]C. L. Chen, C. C. Leiby, and L. Goldstein, Phys. Rev. 121, 1391 (1961).
[9]P. Sprangle and R. A. Smith, Phys. Rev. A 21, 293 (1980), and references therein.
[10]P. F. Browne, Astrophys. J. 134, 963 (1961).
[11]P. F. Browne, Astrophys. J. 136, 442 (1962).
[12]R. Q. Twiss, Aust. J. Phys. 11, 564 (1958).
[13]R. Q. Twiss, Astrophys. J. 136, 438 (1962).

## Nonrandom Suprathermal Electron Emission in Resonance Absorption

Paul Kolodner[a] and Eli Yablonovitch[b]
*Gordon McKay Laboratory, Harvard University, Cambridge, Massachusetts 02138*
(Received 29 July 1980)

Evidence is reported for a nonrandom process by which laser-produced plasmas emit suprathermal electrons. Emission is dominated by a 1 to 2 psec monoenergetic burst, during which the electron energy decreases rapidly. The suprathermal tail on the energy distribution is due to the integrated temporal variation of the electron energy, not to statistical processes. The hot-electron temperature thus produced is practically independent of laser pulse energy.

PACS numbers: 52.50.Jm

Hot-electron production in laser-produced plasmas is a crucial issue in laser fusion research. Electrons heated by "wave breaking" and resonance absorption (RA) have been predicted in computer simulations,[1] inferred from hard x-ray spectra,[2] and directly observed in gaseous targets.[3] They form a suprathermal tail, of temperature $T_h$, on the plasma electron energy distribution. In simulations,[1] $kT_h$ is found to coincide with the wave-breaking energy, given by the well-known formula[4]

$$\mathcal{E}_{\rm br} = eE_d L_{\rm br}\,, \qquad (1)$$

where $E_d$ is the driving electric field, and $L_{\rm br}$ is the density-gradient scale length in the critical layer. But the mechanism by which long-mean-free-path electrons come to be emitted with a broad energy spectrum is still unclear. A recent suggestion[5] is that electrons are emitted in a monoenergetic burst every optical cycle, but that, because of the fluctuating phase of the driving field, $\mathcal{E}_{\rm br}$ fluctuates from cycle to cycle. Thus, after some time (many picoseconds, for $\lambda = 10.6$ $\mu$m), a broad spectrum is created. In this model, the plasma density structure is determined by the ponderomotive force of the laser light.

However, in our experiments with short-rise-time $CO_2$ laser pulses focused onto inhomogeneous gaseous $D_2$ targets, it appears that electron emission lasts less than 20 psec, an insufficient time for strong profile modification[6] or other hydrodynamic motion. We thus propose a model in which the plasma density profile is determined solely by the progress of the laser-driven breakdown wave[7] which rapidly sweeps through the target at the beginning of the laser pulse. On this basis, the driving field, $E_d$, and thus the wave-breaking energy, $\mathcal{E}_{br}$, can be calculated as a function of time. We presume that emission is *monoenergetic* at each instant. We find that, after ionization starts to build up in the underdense region ahead of the critical layer, $E_d$ decreases rapidly, causing $\mathcal{E}_{br}(t)$ to drop out of the experimentally observable range within a few picoseconds after critical-layer breakdown. On this time scale (only a few tens of optical cycles), even the randomization mechanism of Ref. 5 may not be able to produce a broad energy spectrum. However, we find that the spectrum of the integrated temporal variation of $\mathcal{E}_{br}(t)$ has properties which match our experimental observations.

Our experiment consists of irradiating, with $CO_2$ laser pulses of various shapes, a shock front produced in a $D_2$-filled electrothermal shock tube, as discussed in a forthcoming publication.[8] Ionization of the shock-front density step by a laser-driven breakdown wave[7] creates a plasma in which the orientation of the critical surface, and hence the fast-electron emission direction, is reproducible. This allows the use of a magnetic-focusing spectrometer of ± 15% energy resolution for direct time-integrated electron energy spectrum measurements. The spectrum for energies between 40 and 140 keV is fitted by a suprathermal tail of temperature $T_h$. Figure 1(a) shows $T_h$ vs laser pulse energy $E_p$ for $CO_2$ laser pulses of peak intensity $I \sim 10^{14}$ W/cm$^2$, rise time 220 psec, and full width at half maximum (FWHM) 500 psec. We find $T_h \propto E_p^{\delta}$ with $\delta = 0.32 \pm 0.03$, in agreement with computer simulations of RA accompanied by strong profile modification.[9] We view this agreement as evidence against systematic experimental artifacts. However, our laser system is also capable[10] of producing pulses with 20-psec rise time and adjustable fall time, allowing pulse durations of 100–200 psec FWHM. Figure 1(b) shows that these pulses produce a much weaker scaling, $\delta = 0.1 \pm 0.1$, in contradiction with Ref. 9. Also, $T_h$ is independent of the duration of the tail of the laser pulse, leading to the conclusion, mentioned above, that emission takes place only during the 20-psec rise time. Two other important observations are that $T_h$ depends only weakly on shock-tube pressure (which determines the neutral-shock-front density-gradient scale length[11]) and that the total number of emitted electrons, typically $\mathcal{N}_t \sim 3 \times 10^9$, appears space-charge limited in accordance with the Langmuir-Child law. We are unable to reconcile these observations with the theory of ponderomotive profile steepening.

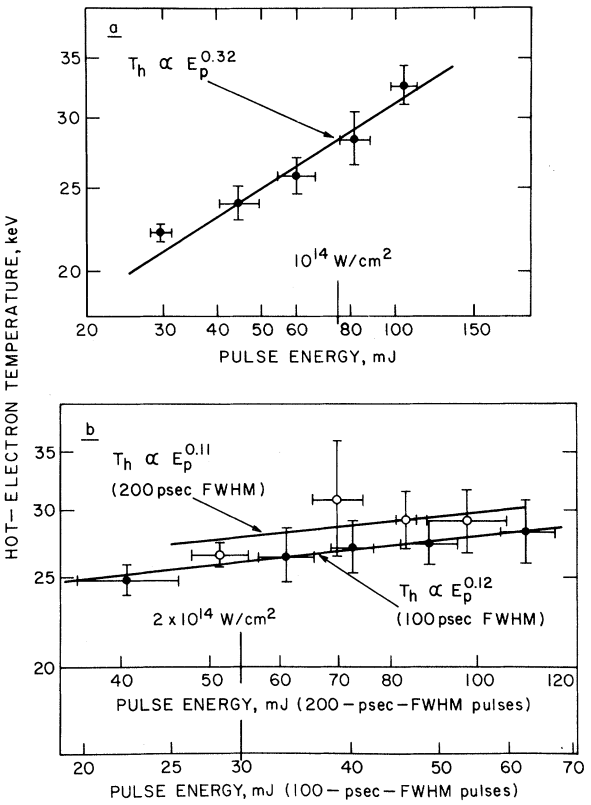


FIG. 1. Hot-electron temperature vs laser pulse energy produced in shock fronts in $D_2$. Markers calibrate the horizontal axes to peak intensity. (a) 220-psec-rise-time pulses; $D_2$ pressure 43–45 Torr. (b) 20-psec-rise-time pulses; $D_2$ pressure 43–67 Torr. Closed circles: 100-psec FWHM. Open circles: 200-psec FWHM.

In our numerical calculation, target breakdown is determined by the avalanche ionization scaling laws.[12] The ionization rate is set proportional to the laser intensity. The density of ionizing collision partners is set equal to the initial atomic density until ionization is complete. Hydrodynamic motion is ignored. The laser pulse has a 20-psec rise time, and its energy is calibrated against experimentally measured breakdown

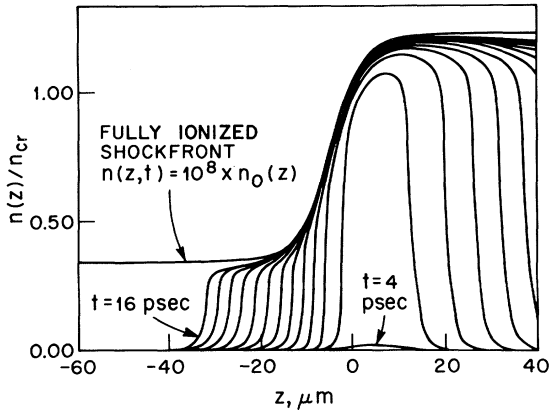


FIG. 2. Calculated plasma density, $n(z)/n_{cr}$, vs distance, $z$, for irradiation of a shock front with $M=5.1$ in 53-Torr $D_2$ by a 100-mJ, 20-psec–rise-time laser pulse. The different profiles are separated in time by 1 psec.

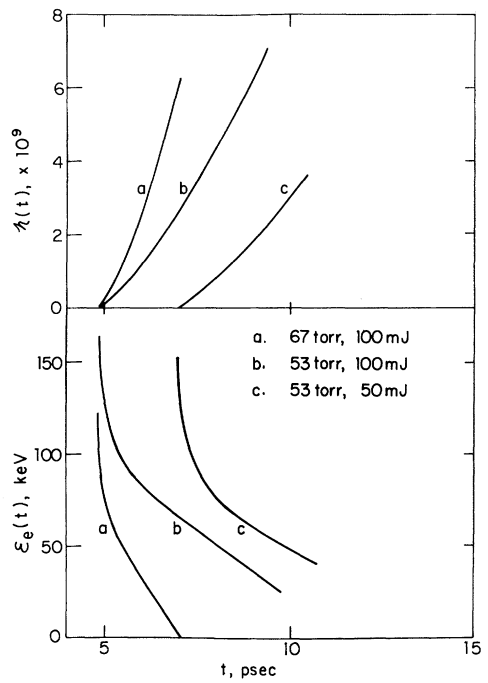


FIG. 3. Calculated integrated number, $\mathfrak{N}(t)$ (top), and emitted energy, $\mathcal{E}_e(t)$ (bottom), of electrons produced in shock fronts irradiated by 20-psec–rise-time laser pulses, vs time.

thresholds. The un-ionized shock-front density profile is calculated from previously published data.[11] The initial electron density in the shock front is set at $10^{11}$ cm$^{-3}$, as determined experimentally with Langmuir probes. Numerical integration of the ionization rate yielded the family of plasma density profiles shown in Fig. 2. Here, the 100-mJ laser pulse was focused, from the left, onto the point $z=0$, with focal depth $z_0=21$ μm. The target was a Mach-5.1 shock front in 53-Torr $D_2$. The ionization builds up very rapidly near the focus. A critical surface is formed at $t=4.9$ psec; at that time, the critical-layer density-gradient scale length is very long. The ionization front then propagates towards the laser with velocity $\sim 3\times 10^8$ cm/sec, in agreement with experimental observations.[13]

Laser-light tunneling into the critical surface is crudely accounted for by approximating the curves in Fig. 2 as linear density ramps of time-varying scale length

$$L_t(t)=(2/n_{cr})\int_{-\infty}^{z_{cr}(t)} n(z,t)\,dz, \qquad (2)$$

where $z_{cr}(t)$ is defined by $n(z_{cr},t)=n_{cr}$. [$L_t(t)$ is *not* the same as $L_{br}$ in Eq. (1)]. The driving field for Eq. (1) is then given by[4]

$$E_d(t)=1.2E_0/[2\pi k_0 L_t(t)]^{1/2}, \qquad (3)$$

where $E_0$ is the vacuum electric field of the laser. Equations (1)–(3) thus determine the instantaneous value of $\mathcal{E}_{br}(t)$. The number of electrons accelerated during a given time interval is calculated by assuming that a certain fraction, $f$, of the laser energy incident during that interval is converted into electrons of energy $\mathcal{E}_{br}(t)$. Removing an integrated number $\mathfrak{N}(t)$ of electrons leaves the target with a space-charge potential $\Phi_p(t)\propto\mathfrak{N}(t)\propto f$. Electrons created with energy $\mathcal{E}_{br}(t)$ escape the target with energy $\mathcal{E}_e(t)=\mathcal{E}_{br}(t)-e\Phi_p(t)$.

Figure 3 shows the temporal behavior of $\mathfrak{N}(t)$ and $\mathcal{E}_e(t)$, for three typical experimental situations. At the instant of breakdown, $L_{br}$ is very large, and thus so is $\mathcal{E}_e(t)$. Very rapidly, however, the underdense side of the shock front is ionized, and so $L_t(t)$ grows. Thus the evanescent field $E_d$ drops rapidly, and so does $\mathcal{E}_e(t)$. After some time, the buildup of the space-charge potential $\Phi_p(t)$ causes $\mathcal{E}_e(t)$ to drop to 0, and emission stops. Figure 3 illustrates two important points. First, electrons collected in our experiment (40 keV $<\mathcal{E}_e<$ 140 keV) are emitted in a burst lasting only 1 to 2 psec. 30 to 60 optical cycles is not enough time for the random process of Ref. 5 to produce a complete, broad spectrum. Rather, that process is only expected to introduce in these curves a small amount of noise which, when integrated in time, has little effect on the energy spectrum. Randomness plays no role here. Second, the effect of changing experimental conditions is simply to displace the curves

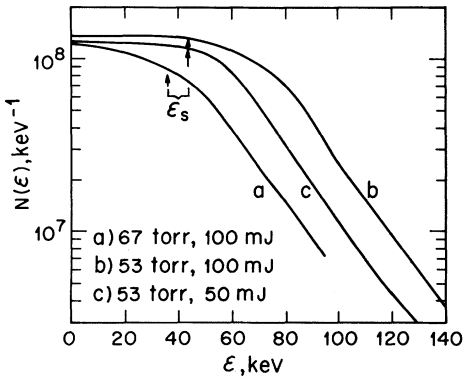


FIG. 4. Energy spectra of electrons emitted as in Fig. 3. The spectrum starts to fall off in a suprathermal tail roughly at energy $\mathcal{E}_s$.

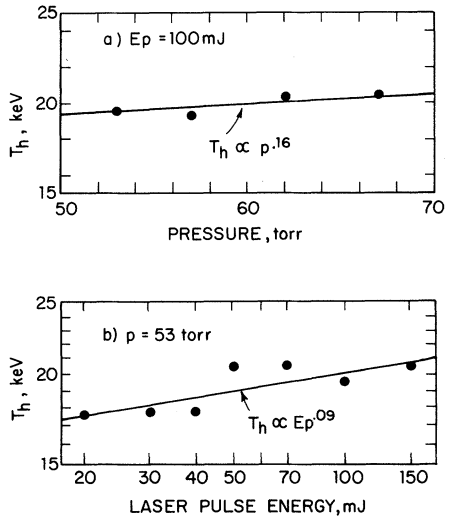


FIG. 5. Calculated scaling of hot-electron temperature, $T_h$, with shock-tube pressure, $p$ (top), and laser pulse energy, $E_p$ (bottom).

of Fig. 3 on the graph, with little change in shape for $\mathcal{E}_e \gtrsim 50$ keV. This has little effect on the temperature, $T_h$, of the high-energy part of the resulting spectrum. This is in agreement with our experimental observations.

Figure 4 shows the actual energy spectra, $N(\mathcal{E})$, determined by the curves of Fig. 3. $N(\mathcal{E})$ is flat out to an energy $\mathcal{E}_s$ and then drops off in a remarkably straight suprathermal tail. The effect of varying the parameter $f$ may be roughly described as a displacement of the curves along a diagonal of the graph. Varying $f$ from 0.05 to 1.0 has little effect on the slope of the tail ($T_h$) or on the total number, $\mathfrak{N}_t = \int_0^\infty N(\mathcal{E})\,d\mathcal{E}$, of emitted electrons. In this model, the *total* electron emission is space-charge limited, but this does not affect $T_h$. These features are observed experimentally. The model predicts $\mathfrak{N}_t \sim (6 \text{ to } 12) \times 10^9$, about a factor of 2 larger than the experimental value.

As shown in Fig. 5, the exponents in the scaling of the calculated values of $T_h$ with experimental parameters are in remarkable agreement with experimental values. This is felt to be a confirmation of the applicability of the model to the experiment. The actual magnitude of $T_h$ is smaller than seen experimentally; this is due to the crude accounting of the tunneling of the electric field through the underdense plasma. A virtue of this model is that its major results are independent of the values of any free parameters.

To summarize, in our model, the plasma density profile is due solely to fast avalanche ionization. This causes electron emission in a burst which is too short to be influenced by random processes. The electron energy spectrum is thus due to the integrated temporal variation of the electron energy and depends weakly on experimental parameters. This mechanism may be active during the initial stage of breakdown of any laser target and can allow substantial high-energy electron emission before space-charge limitations set in. A more detailed account of this work will soon be published.

We thank Jerry Black for maintaining the laboratory microcomputer on which these calculations were performed. This work was supported by the U. S. Department of Energy.

---

[a]Present address: Bell Laboratories, Murray Hill, N. J. 07974.

[b]Present address: Exxon Research and Engineering, Linden, N. J. 07036.

[1]J. P. Friedberg, R. W. Mitchell, R. L. Morse, and L. I. Rudsinski, Phys. Rev. Lett. 28, 795 (1972).

[2]J. F. Kephart, R. P. Godwin, and G. H. McCall, Appl Phys. Lett. 25, 108 (1974).

[3]P. Kolodner and E. Yablonovitch, Phys. Rev. Lett. 37, 1754 (1976).

[4]V. L. Ginzburg, *Propagation of Electromagnetic Waves in Plasmas* (Pergamon, New York, 1964).

[5]B. Bezzerides, S. J. Gitomer, and D. W. Forslund, Phys. Rev. Lett. 44, 651 (1980).

[6]J. S. DeGroot and J. E. Tull, Phys. Fluids 18, 672 (1975).

[7]Yu P. Raizer, Zh. Eksp. Teor. Fiz. 48, 1508 (1965) [Sov. Phys. JETP 21, 1009 (1965)].

[8]P. Kolodner and E. Yablonovitch, to be published.

[9]D. W. Forslund, J. M. Kindel, and K. Lee, Phys.

Rev. Lett. 39, 284 (1977); K. Estabrook and W. Kruer, Phys. Rev. Lett. 40, 42 (1977).
[10]H.-S. Kwok and E. Yablonovitch, Appl. Phys. Lett. 30, 158 (1977).
[11]H. Ahlsmeyer, J. Fluid. Mech. 74, 497 (1976).
[12]E. Yablonovitch, Appl. Phys. Lett. 23, 121 (1973).
[13]H.-S. Kwok, Ph.D. thesis, Harvard University, 1978 (unpublished).

# Profile Modification and Hot-Electron Temperature from Resonant Absorption at Modest Intensity

J. R. Albritton and A. B. Langdon
*University of California, Lawrence Livermore Laboratory, Livermore, California 94550*
(Received 17 April 1980)

Resonant absorption is investigated in expanding plasmas. The momentum deposition associated with the ejection of hot electrons toward low density via wave breaking readily exceeds that of the incident laser radiation and results in significant modification of the density profile at critical density. New scaling of hot-electron temperature with laser and plasma parameters is presented.

PACS numbers: 52.50.Jm

Theory indicates that lasers of current application may be expected to exhibit significant collisionless interaction with inertial-confinement fusion targets. Here we consider resonant absorption[1] which acts at critical density where the laser frequency equals the local electron plasma frequency. Because the dominant laser-plasma coupling occurs near critical density, it is essential to develop a self-consistent description of the dynamics there. It will be seen that even weak resonant absorption acts strongly upon the hydrodynamical evolution of this region so as to enhance itself and suppress other mechanisms.

Resonant electron oscillations transfer absorbed energy to the plasma by ejecting particles toward low density via wave breaking.[1] *The associated momentum deposition readily exceeds that of the driving laser radiation.* These hot collisionless electrons are confined by the electrostatic potential and subsequently pose two challenges to laser fusion: (1) to prevent them from preheating the target and (2) to use their energy to drive its implosion.

Implosion experiments at *modest* intensity are already in progress[2] to increase the density of the compressed core above that of *high*-intensity exploding-pusher target experiments[3] which are strongly preheated by hot electrons from resonant absorption. The scaling of hot-electron temperature in the high-intensity regime is the subject of recent theoretical work[4,5]; briefly, the laser beam or driven wave steepens the density profile at critical density and thereby reduces the rate of increase of the hot-electron temperature with increasing laser intensity from estimates based on the usual coronal rarefaction.

Here we report new and improved scaling laws for the temperature of hot electrons produced by resonant absorption in the modest intensity regime. (We will, in fact, argue for the general validity of our results.) *The dependence of hot-electron temperature upon background cold-electron temperature is shown to be as strong as that upon laser intensity.*

The interaction of modest-intensity 1.06-$\mu$m laser radiation with high-$Z$ disc targets has been modeled by *ad hoc* strong limitation of electron energy conduction.[6] The resulting coronal rarefaction exhibits a step in density including critical and hot plasma below the subcritical density at which the flow emerges from the step. Most interaction mechanisms are suppressed in such a profile.

In fact, resonant absorption is enhanced in a self-consistent stepped density profile.[1,4,5,7] *Here we provide a first principles model of profile modification in the modest-intensity regime as the local response of the flow to the momentum deposited at critical density by hot-electron production.*

The upper density of the induced step may be much greater than critical density and much greater than that associated with radiation-pressure steepening. Experimental observations of such structures have been reported recently.[8] The associated lower density and absence of an extensive turning region act to suppress inverse bremsstrahlung and stimulated Brillouin scattering. The step in electrostatic potential associated with the density step contributes to the formation

 